Synthesis of Hybrid Polyaniline/Carbon Nanotube Nanocomposites by Dynamic Interfacial Inverse Emulsion Polymerization Under Sonication

R. Y. Suckeveriene, E. Zelikman, G. Mechrez, A. Tzur, I. Frisman, Y. Cohen, M. Narkis

Department of Chemical Engineering, Technion-IIT, Haifa, Israel

Received 2 June 2010; accepted 16 August 2010
DOI 10.1002/app.33212
Published online 21 October 2010 in Wiley Online Library (wileyonlinelibrary.com).

ABSTRACT: This article describes an ultrasonically assisted *in situ* interfacial dynamic inverse emulsion polymerization process of aniline in the presence of multiwalled carbon nanotubes (MWNT) in chloroform. During polymerization, MWNT are coated with polyaniline (PANI) forming a core-shell structure of nanowires, as evidenced by cryogenic transmission electron microscopy. Thermogravimetric analysis curves and conversion measurements provided important knowledge regarding the unique polymerization method. Scanning electron microscopy images and surface resistivity imply that PANI/MWNTs are characterized by a structural synergistic effect. The PANI coating of MWNT leads to a remarkable improvement in separation and dispersion of MWNT in chloroform, which otherwise would rapidly coagulate and settle. The presented interfacial dynamic polymerization process is very fast, reaching 82% conversion within 5 min of sonication and produces stable clear dispersions of doped PANI in chloroform. © 2010 Wiley Periodicals, Inc. J Appl Polym Sci 120: 676–682, 2011

Key words: conjugated polymers (polyaniline); carbon nanotubes; thin films; thermogravimetric analysis (TGA); polymer synthesis and characterization

INTRODUCTION

Polymeric nanocomposites consist of nanoparticles imbedded in organic polymers comprising a new class of materials. Homogeneous dispersions of nanoparticles in polymers using conventional processing techniques are difficult to produce because nanoparticles tend to agglomerate. Thus, efficient methods for agglomerate breakdown have been sought in recent years. Researchers have focused on methods of *in situ* polymerization of monomers in the presence of carbon nanotubes (CNTs) such as sol–gel and intercalation polymerization processes.[1–6] Many reports appear in the literature regarding CNTs, polymerization of aniline, preparation of polyaniline (PANI)/CNT nanocomposites, and various applications, including thin, transparent, and electrically conductive films.[5–11]

Emulsion polymerization is a process used for radical chain polymerization in systems comprising water, monomers, and surfactants. The monomers polymerize within micelles and form stable colloidal dispersions, i.e., emulsions.[12] Emulsion polymerization can also be carried out by an inverse emulsion polymerization procedure. Here, the continuous phase is the organic phase containing the monomer, while the aqueous solution containing the surfactant and initiator is emulsified by the surfactant. Inverse emulsion polymerization can be used for various monomers, including aniline.

CNTs have drawn much attention in recent years, since their first observation by Iijima.[13] CNTs possess a remarkable combination of properties, i.e., high strength and stiffness along with flexibility accompanied with high electrical and thermal conductivity, thus offering opportunities for development of new nanocomposites.[7] Because CNTs have poor "solubility" in most solvents and poor compatibility with polymeric matrices, fine dispersions are difficult to achieve.

PANI is one of the most studied conducting polymers because of its simple preparation, high conductivity, and environmental stability.[14] Many production methods of PANI are reported in the literature, as described by MacDiarmid et al.[15]: "there are as many different types of PANI as there are people synthesizing it." Indeed there are many methods for production of PANI: in organic, or aqueous phase, using agitation or sonication methods, static interfacial, emulsion, and inverse emulsion polymerization. The following section provides a brief description of the various approaches for preparation of PANI/CNT nanocomposites.

Correspondence to: M. Narkis (narkis@tx.technion.ac.il).

Contract grant sponsors: Miriam and Aaron Gutwirth Memorial Fellowship Fund; Magnet Program, Israel Ministry of Trade and Industry, NES Consortium; Russell Berrie Nanotechnology Institute (RBNI), Technion.

Ginic-Markovic et al.[7] described a method of ultrasonic emulsion polymerization of aniline in the presence of CNTs. This process decreases agglomeration of CNTs, creating a micelle structure around the CNTs, which becomes "soluble" in water for a certain period of time. This *in situ* polymerization method allows the production of wrapped and stabilized nanotubes by PANI.

Konyushenko et al.,[16] Guo and Li,[17] and Zhang et al.[18] also described multiwalled CNTs (MWNT) coating with PANI via an *in situ* polymerization method. There are several methods of production of PANI, one of which presented by Soares et al.[19] describes an inverted emulsion polymerization method of aniline in toluene.

In this article, a new sonicated *in situ* inverse emulsion polymerization method of aniline is described. The reaction conducted in the presence of the MWNTs is very fast, resulting in PANI-coated MWNTs, which exhibit improved properties.

EXPERIMENTAL

Materials

Aniline monomer was used after purification (Aldrich, St. Louis, MO). (±)Camphor-10-sulfonic acid (β) (CSA) (Riedel de-Haën, Sigma-Aldrich, Germany) was used as received without further purification. Chloroform was used as the solvent (Bio Lab Ltd., Israel). The studied Nanocyl 7000 MWNT has an average diameter of 9.5 nm and average length of 1.5 μm (Nanocyl, Belgium). Ammonium peroxydisulfate (APS) was used as received (Riedel de-Haën, Sigma-Aldrich).

Preparation of nanocomposites

The inverse emulsion polymerization procedure of aniline in chloroform is conducted as shown in Figure 1: a certain amount of surfactant (CSA) is dissolved in 20 mL chloroform using magnetic stirring. Different concentrations of distilled aniline are added, and a clear solution is formed. Vibra cell VCX 750 (Sonics and Materials Inc., Newtown, CT) ultrasonic liquid processor was used to disperse the MWNT during polymerization. MWNT is added in two ways: (a) *in situ* where the MWNT is added before polymerization begins and (b) *ex situ* where MWNT is added after the polymerization process ends. MWNT concentration is usually 0.1 wt % of the aniline. Sonication to disperse the CNTs in the chloroform/aniline solution takes about 1 min. APS dissolved in 1 mL distilled water is added to the chloroform/aniline solution followed by sonication at 4°C for 1–9 min. The PANI/CNT dispersion is then used for film formation using an air brush instrument or coating rods. A reference sample without MWNT is prepared using the same procedure. The molar ratios of aniline : CSA : APS are 1 : 1 : 1, or 1 : 1 : 0.25, respectively.

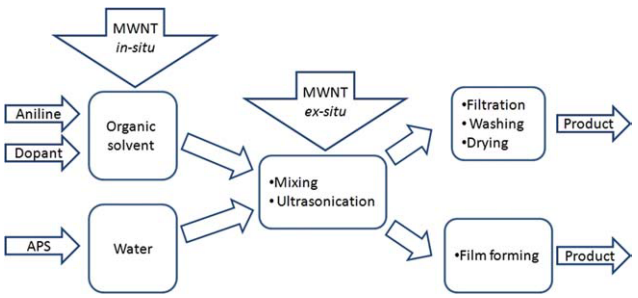

Figure 1 Schematic illustration of the polymerization procedure. [Color figure can be viewed in the online issue, which is available at wileyonlinelibrary.com.]

The polymerization conversion is determined as follows: the mass of polymerization is transferred to a 250-mL beaker and chloroform is evaporated. A solution of 50 mL H_2O and 50 mL NH_4OH (ammonium hydroxide) is added to the PANI dispersion, where the acid reacts with the base, resulting in a dedoped PANI. The aqueous phase is removed using a gravitational filtration, followed by washing with H_2O and drying in a vacuum oven for 2 hr. The conversion is calculated using eq. (1).

$$\text{Conversion}(\%) = W_{\text{dedoped PANI}}/W_{\text{aniline}} \times 100 \quad (1)$$

Characterization

The PANI/CNT nanocomposite's morphology was studied using scanning electron microscopy (SEM; Philips XX20, model D816). Thermal analysis was performed using a TA 2050 thermogravimetric analyzer. Samples were heated under air, at a rate of 20°C/min, monitoring their weight loss as a function of temperature. Two types of information can be extracted from the thermogravimetric analysis (TGA) thermograms: (a) the degradation temperature regions of the acid and polymer fractions, normally within 200–350°C and 400–700°C, respectively, and (b) the nanotube's fraction. A four-point probe technique is used to measure the electrical conductivity at conductivity levels higher than 10^{-4} S/cm.

Transmission electron microscopy (TEM) micrographs were obtained for ultrafast cooled vitrified cryo-TEM specimens prepared under controlled conditions of 20°C and 100% relative humidity as described elsewhere.[20] Specimens were examined in a Philips CM120 cryo-TEM operating at 120 kV, using an Oxford CT3500 cooling-holder system at about −180°C. Low electron-dose imaging was performed with a Gatan Multiscan 791 CCD camera, using the Gatan Digital Micrograph 3.1 software package.

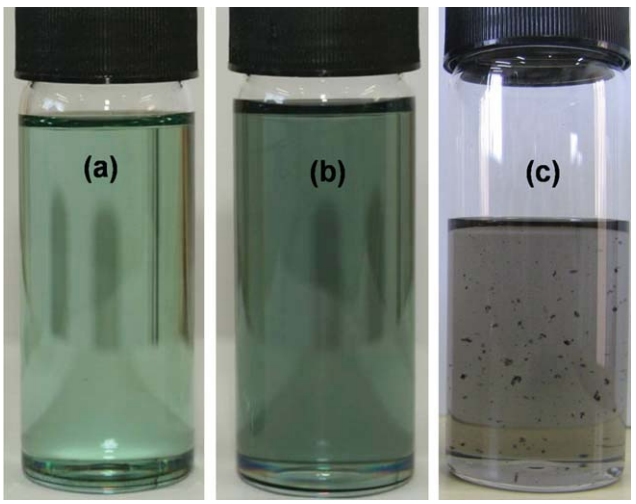

Figure 2 Dispersions in chloroform of (a) PANI, (b) PANI/MWNT, and (c) neat MWNT. [Color figure can be viewed in the online issue, which is available at wileyonlinelibrary.com.]

Absorbance Fourier-transform infrared (FTIR) spectra were recorded using a Nicolet Thermo 6700 FTIR instrument equipped with a Smart iTR diamond ATR device. Each spectrum was recorded at a resolution level of 4 cm^{-1}.

RESULTS AND DISCUSSION

Figure 2 demonstrates two clear dispersions of (a) PANI and (b) PANI/MWNT in chloroform prepared as previously described. The dispersions were stable for long periods of time without any visible precipitation. Neat CNTs dispersed in chloroform with CSA rapidly coagulate and settle as shown in Figure 2(c), similar to previous reports.[6,21]

Figure 3 depicts FTIR spectra of dedoped PANI, known as emeraldine base. The emeraldine base has characteristic FTIR peaks, as reported elsewhere[22]: at $\sim$ 1590 and $\sim$ 1497 cm^{-1}, which represent the C=C

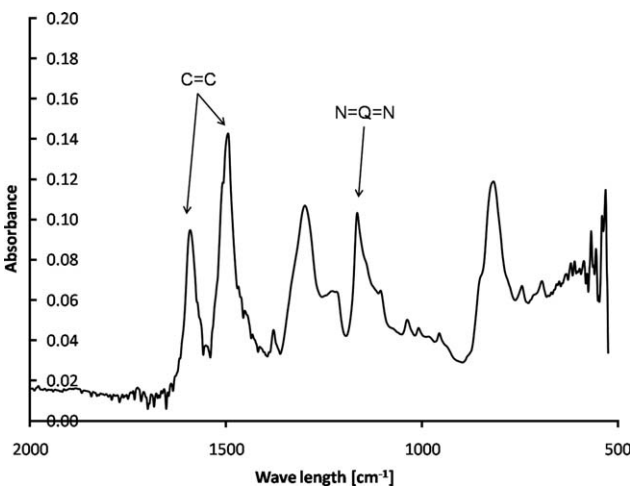

Figure 3 FTIR spectrum of dedoped PANI.

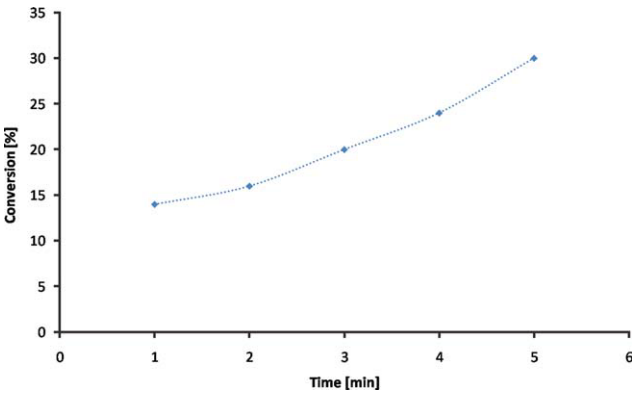

Figure 4 Conversion as a function of polymerization period. [Color figure can be viewed in the online issue, which is available at wileyonlinelibrary.com.]

stretching vibrations of quinoid and benzenoid rings, respectively. The peak at $\sim$ 1160 cm^{-1} represents N=Q=N, where Q is the quinoid ring. The appearance of these peaks confirms that the unique dynamic sonication inverse emulsion polymerization has resulted in PANI.

Figure 4 depicts conversion as a function of polymerization time, where the molar ratios are aniline : CSA : APS = 1 : 1 : 0.25. A maximum conversion, of 64%, was obtained by static polymerization, without sonication, where polymerization took place at the interphase region between the organic and aqueous phases, after 45 days at room temperature. An outstanding result is the extremely fast polymerization process under the ultrasonic field where the conversion was $\sim$ 30% after only 5 min. Further studies of conversion as function of the system's parameters has led to fast, very high conversions as is shown in Figure 5. The present inverse emulsion polymerization process can be described as a fast dynamic interfacial polymerization process, in which tiny water dispersed droplets containing APS formed by the ultrasonic field meet the continuous chloroform medium containing aniline and CSA. At the

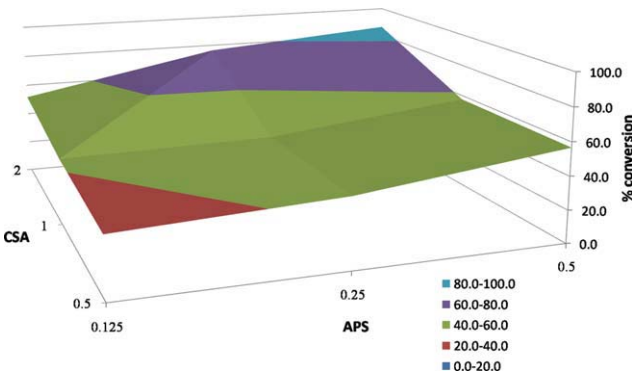

Figure 5 Conversion as a function of CSA and APS at different molar ratios. [Color figure can be viewed in the online issue, which is available at wileyonlinelibrary.com.]

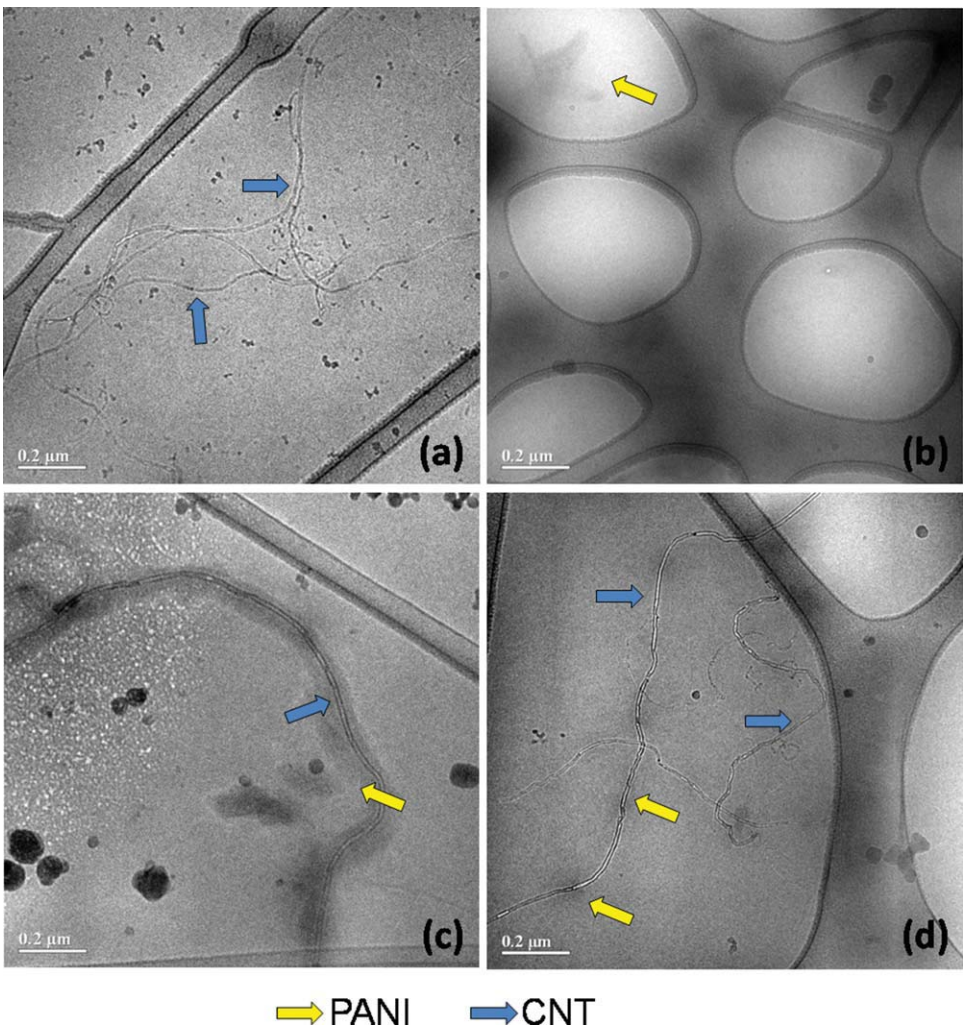

Figure 6 Cryo-TEM of (a) neat MWNT, (b) neat PANI, (c) PANI/MWNT *in situ*, and (d) PANI/MWNT *ex situ*. [Color figure can be viewed in the online issue, which is available at wileyonlinelibrary.com.]

interfaces, APS radicals in the aqueous droplets collide with the aniline/CSA (anilinium) complex dispersed in the organic phase; thus, PANI forms at the interfaces. Because a lot of interface is available, the polymerization rate is very fast. Moreover, the high-powered ultrasonic radiation field assists in the creation of free radicals, thus, further contributing to the acceleration of the polymerization process.[7] Contrary to the described fast process, inverse emulsion polymerization in the absence of sonication[19] and static interfacial polymerization[23] is very slow.

Figure 5 depicts conversion as a function of the initial molar ratios of CSA and APS related to aniline, for polymerization periods of 5 min dynamic followed by 30 min static each. As APS concentration increases, so does conversion, presumably owing to higher concentrations of radicals, which increases the polymerization rate. Moreover, as CSA concentration increases, so does conversion. The polymerization of aniline is dependent on the acidity of the system.[14] The initial oxidation step is always linked to the oxidation of neutral aniline molecules, whereas short oligomers (containing phenazine) may act as initiation centers for the subsequent polymerization process. When the acidity is high (pH < 2.5), the oligomers formed result in the formation of initiation centers, thus increasing the polymerization rate. A maximal conversion after 5 min sonication of $\sim$ 82% was obtained when the concentrations of both APS and CSA were the highest.

Figure 6 depicts cryo-TEM micrographs of (a) neat MWNT, (b) neat PANI, (c) PANI/MWNT *in situ*, and (d) PANI/MWNT *ex situ*. Figure 6(a) shows a small bundle of MWNT, with an average MWNT diameter of $\sim$ 10 nm, indicating poor dispersion of the MWNT in chloroform. The dark areas in Figure 6(b) are presumably neat PANI in chloroform. Figure 6(c) (*in situ*) shows a single MWNT uniformly coated with PANI, with an average diameter of $\sim$ 50 nm, Similar results were observed using high-resolution SEM[6] and also reported elsewhere.[6,7,16–18] Figure 6(d) (*ex situ*) shows several MWNT with local darker

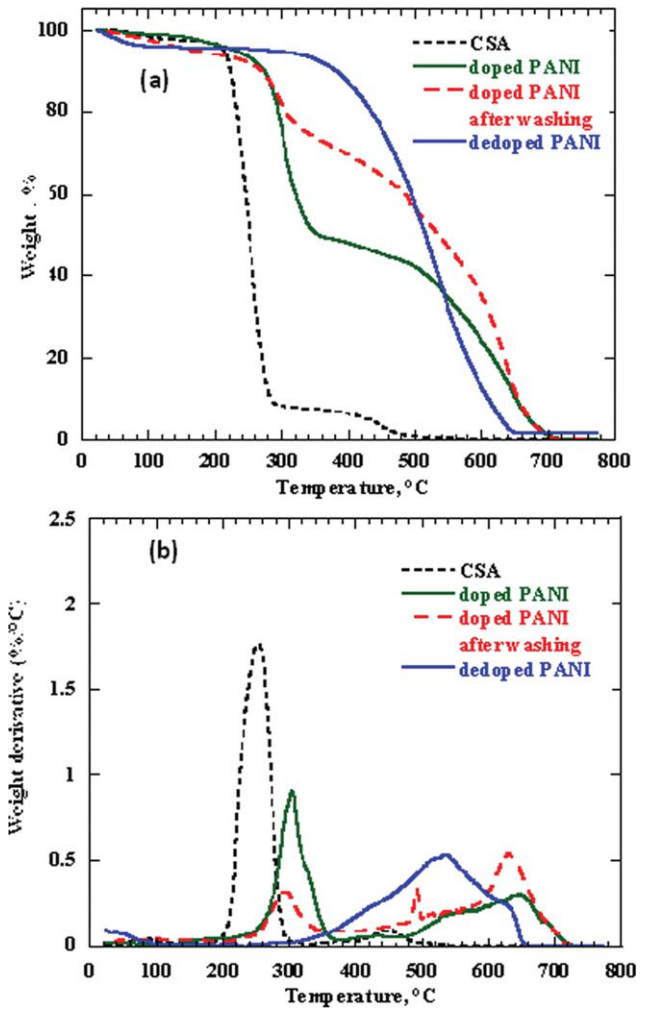

Figure 7 TGA and DTG thermograms in air of neat CSA, doped PANI, water-washed doped PANI, and dedoped PANI. [Color figure can be viewed in the online issue, which is available at wileyonlinelibrary.com.]

areas indicating discontinuous PANI coating along the nanotube. Similar to a work reported elsewhere,[24] it is suggested that PANI interacts and coats the CNT. Both PANI/MWNT *in situ* and *ex situ* have produced stable dispersions for long periods of time. Thus, PANI acts as a stabilizer for the MWNT by interactions with the MWNT surfaces, as shown in Figure 6(c,d).

Figure 7 depicts TGA and DTG thermograms in air of neat CSA, doped PANI, doped PANI after washing with distilled water, and dedoped PANI. The TGA curves show that dedoped PANI has a single decomposition stage, whereas both doped PANI and washed doped PANI exhibit two decomposition stages. The DTG curves show that the neat CSA exhibits a single peak at 251.9°C and the dedoped PANI exhibits a single peak at 534.2°C. However, the doped PANI and the doped PANI after washing exhibit two peaks: initially at 303°C and 294.4°C, respectively, (decomposition of CSA) and then at 648.4°C and 629.4°C, respectively (decomposition of the dedoped PANI). It seems that the higher thermal stability of the doped PANI is due to interaction of PANI with CSA. The TGA curve of doped PANI shows that the CSA weight loss up to ~ 300°C is roughly 50%, whereas the weight loss of the washed doped PANI is less, approximately 30%. Because the polymerization process was usually conducted with excess CSA, part of it is attached to the polymeric chains, whereas the other part remains free. Thus, the 30% weight loss of the washed doped PANI roughly reflects the bound CSA, whereas the 50% weight loss of the dedoped PANI is of bound and free CSA.

Figure 8 depicts TGA and DTG thermograms in air of dedoped PANI at molar ratios of aniline : CSA : APS = 1 : 0.5 : 0.5, 1 : 1 : 0.5, and 1 : 2 : 0.5, i.e., increasing CSA concentrations. The curves exhibit a single decomposition peak, similar to the dedoped PANI shown in Figure 7. The peaks for aniline : CSA : APS = 1 : 0.5 : 0.5, 1 : 1 : 0.5, and 1 : 2 : 0.5 appear at

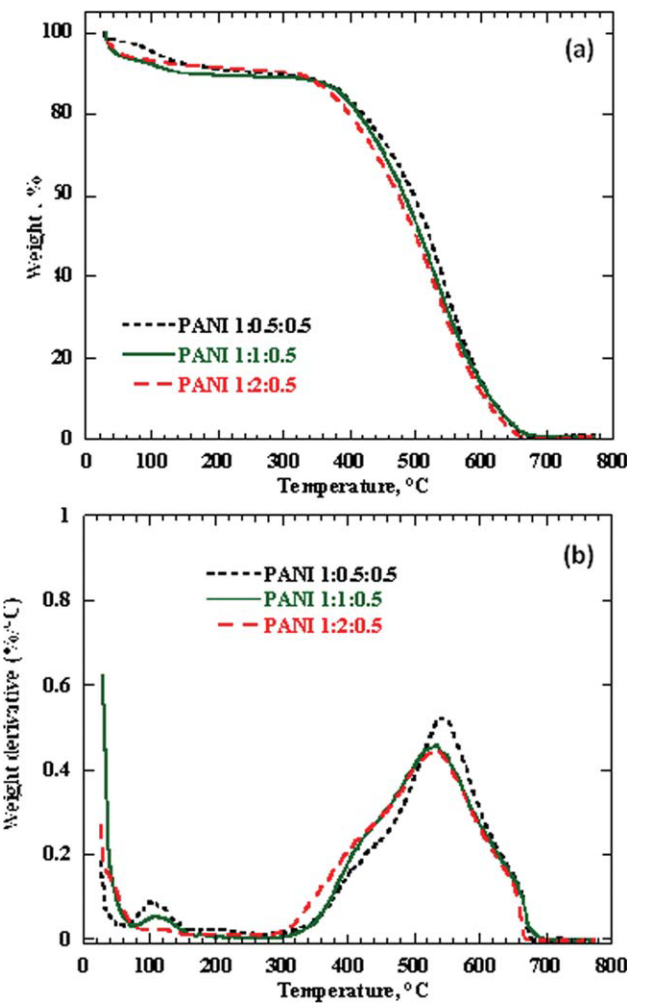

Figure 8 TGA and DTG thermograms in air of dedoped PANI at molar ratios of aniline : CSA : APS = 1 : 0.5 : 0.5, 1 : 1 : 0.5, and 1 : 2 : 0.5. [Color figure can be viewed in the online issue, which is available at wileyonlinelibrary.com.]

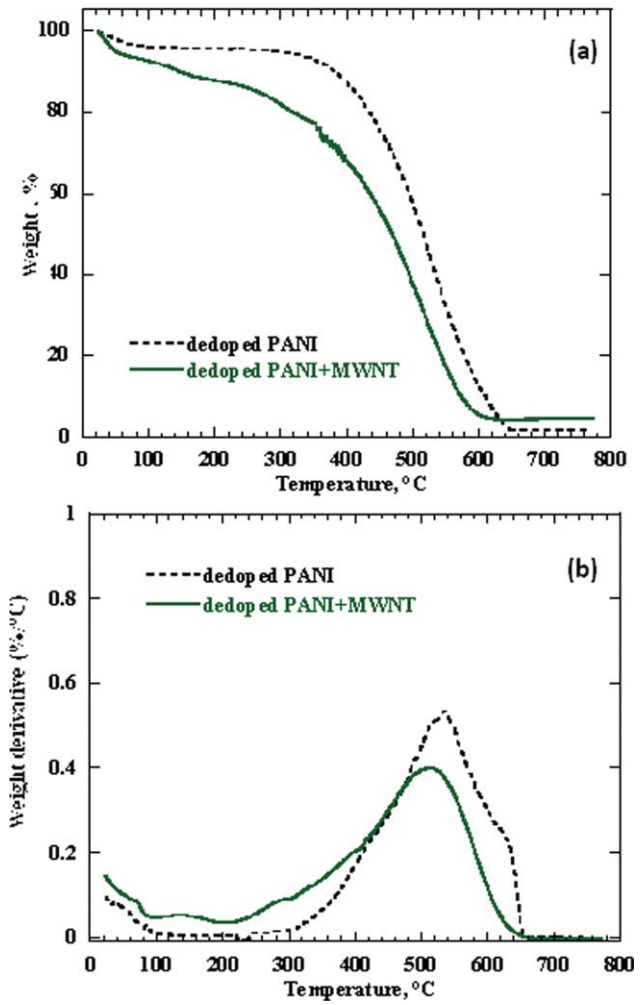

Figure 9 TGA and DTG thermograms in air of dedoped PANI and dedoped PANI/MWNT. [Color figure can be viewed in the online issue, which is available at wileyonlinelibrary.com.]

542.3, 529.2, and 509.9°C, respectively. Presumably, the slight peak reductions as the amount of CSA increases are due to the formation of shorter chain lengths of PANI. As shown in Figure 5, the polymerization rate of aniline increases as the acidity level increases.[14]

Figure 9 depicts TGA and DTG thermograms in air of *in situ* dedoped PANI and dedoped PANI/MWNT. Figure 9(a) shows that, as expected, the dedoped PANI sample fully decomposes, whereas the sample containing MWNT has a residue of ~ 4.5 wt %. The DTG curves [Fig. 9(b)] show that the dedoped PANI has a higher thermal stability, 534.2°C compared with 509.8°C for the PANI/MWNT sample. Because MWNTs are coated with PANI, the interface for oxidation is larger than neat PANI and, therefore, the thermal stability decreases.

Figure 10 depicts thin films of (a) neat PANI, (b) PANI/MWNT, and (c) neat MWNT placed on a glass substrate. Although the neat MWNT [Fig. 10(c)] exhibits a poor film, both PANI films [Fig. 10(a,b)] are uniform and have a transparency of approximately 80% to visible light. Surface resistivity measurements, conducted with the four-point probe, showed that neat PANI and neat MWNT have high resistivities of 222.7 and 334.3 kΩ/□, respectively, whereas the PANI/MWNT exhibited an order of magnitude lower resistivity of 16.9 kΩ/□. The poor conductivity of the MWNT film can be explained by the poor film formation. MWNTs are more conductive than PANI. Because PANI interacts with the MWNT, it reduces the contact resistivity and, thus, increases the conductivity of PANI.

Figure 11 depicts SEM images of (a) neat, (b) PANI, and (c) PANI/MWNT deposited on a porous silica wafer. PANI, Figure 11(b), exhibits a smooth surface, similar to PANI surfaces reported elsewhere[6]; however, it includes numerous voids ranging in size up to ~ 2 μm. The PANI/MWNT film exhibits a rougher surface, however, with no visible voids. These images explain the order of magnitude differences in surface resistivity between the PANI and PANI/MWNT films, as shown in Figure 10. It seems that the PANI/MWNT combination has a

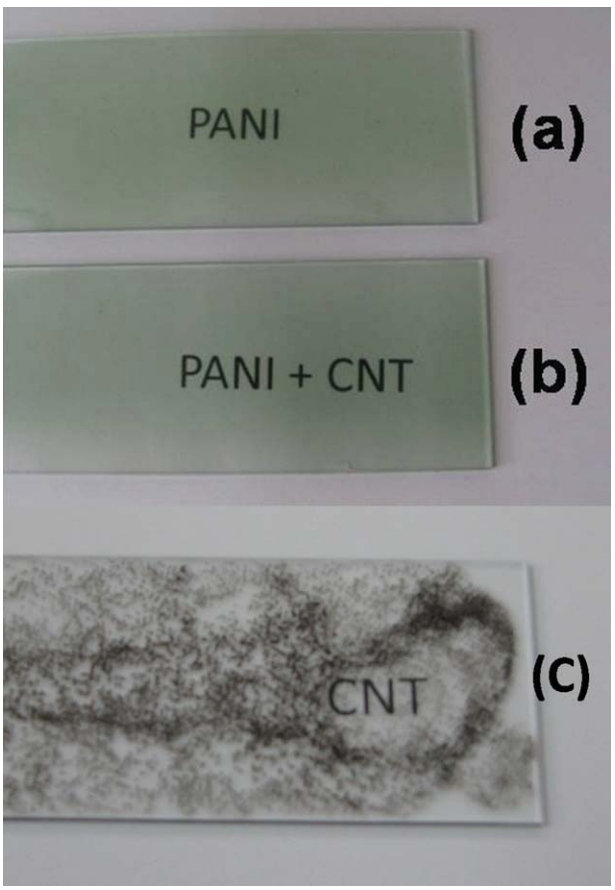

Figure 10 Thin films of (a) neat PANI, (b) PANI/MWNT, and (c) neat MWNT. [Color figure can be viewed in the online issue, which is available at wileyonlinelibrary.com.]

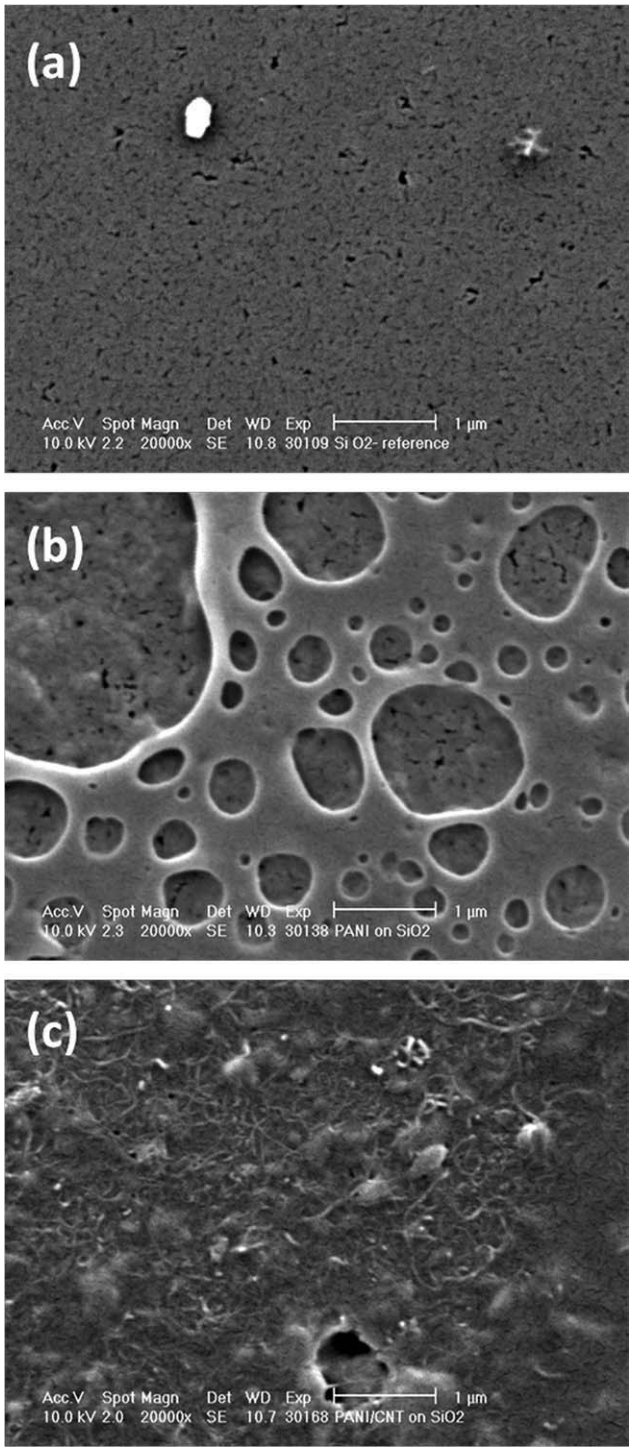

Figure 11 SEM images of (a) neat, (b) PANI, and (c) PANI/MWNT deposited on a SiO_2 porous wafer.

characteristic structural synergistic effect because of interactions between MWNT and the PANI chains, thus, resulting in the full covered surface, leading to increased surface conductivity.

CONCLUSIONS

The described *in situ* dynamic interfacial inverse emulsion polymerization method of aniline was conducted in the presence of MWNT and under sonication, resulting in PANI-coated nanotubes. The dispersions prepared were found to be stable for several months. To the authors' best knowledge, this report is the first one describing the production of stable dispersions of CNT in chloroform. TGA curves and conversion measurements provided some insight regarding the polymerization mechanism. Cryo-TEM images of the composites have shown that the nanotubes are coated with PANI and form a network. SEM images observation and surface resistivity results imply that PANI interacts with the nanotubes and, thus, exhibits synergistic effect. The polymerization method described in this article is simple and very fast compared with the other literature-reported methods. Conversions of up to 82% were achieved within 5 min of dynamic polymerization time.

References

1. Breuer, O.; Sundararaj, U. Polym Compos 2004, 25, 630.
2. Rao, C. N. R.; Mueller, A.; Cheetham, A. K., Eds. The Chemistry of Nanomaterials: Synthesis, Properties and Applications, Vol.1; Wiley-VCH: Weinheim, 2004.
3. Rao, C. N. R.; Mueller, A.; Cheetham, A. K. Eds. The Chemistry of Nanomaterials: Synthesis, Properties and Applications, Vol.2; Wiley-VCH: Weinheim, 2004.
4. Suckeveriene, R. Y.; Tzur, A.; Narkis, M.; Siegmann, A. Polym Compos 2009, 30, 422.
5. Zelikman, E.; Narkis, M.; Siegmann, A.; Valentini, L.; Kenny, J. M. Polym Eng Sci 2008, 48, 1872.
6. Zelikman, E.; Suckeveriene, R. Y.; Mechrez, G.; Narkis, M. Polym Adv Technol 2010, 21, 150.
7. Ginic-Markovic, M.; Matisons, J. G.; Cervini, R.; Simon, G. P.; Fredericks, P. M. Chem Mater 2006, 18, 6258.
8. Jeevananda, T.; Siddaramaiah; Kim, N. H.; Heo, S.-B.; Lee, J. H. Polym Adv Technol 2008, 19, 1754.
9. Kim, D. K.; Oh, K. W.; Kim, S. H. J Polym Sci Part B: Polym Phys 2008, 46, 2255.
10. Vacca, P.; Maglione, M. G.; Minarini, C.; Salzillo, G.; Amendola, E.; Della Sala, D.; Rubino, A. Macromol Symp 2005, 228, 263.
11. Zhang, X.; Zhang, J.; Liu, Z. Appl Phys A Mater Sci Process 2005, 80, 1813.
12. Odian, G. Principles of Polymerization, 4th ed.; John Wiley & Sons: New York, 2004.
13. Iijima, S. Nature 1991, 354, 56.
14. Sapurina, I.; Stejskal, J. Polym Int 2008, 57, 1295.
15. MacDiarmid, A. G.; Jones, W. E.; Norris, I. D.; Gao, J.; Johnson, A. T.; Pinto, N. J.; Hone, J.; Han, B.; Ko, F. K.; Okuzaki, H.; Llaguno, M. Synth Metal 2001, 119, 27.
16. Konyushenko, E. N.; Stejskal, J.; Trchova, M.; Hradil, J.; Kovarova, J.; Prokes, J.; Cieslar, M.; Hwang, J.-Y.; Chen, K.-H.; Sapurina, I. Polymer 2006, 47, 5715.
17. Guo, D.-J.; Li, H.-L. J Solid State Electrochem 2005, 9, 445.
18. Zhang, H.; Li, H. X.; Cheng, H. M. J Phys Chem B 2006, 110, 9095.
19. Soares, B. G.; Leyva, M. E.; Barra, G. M. O.; Khastgir, D. Eur Polym J 2006, 42, 676.
20. Talmon, Y. Surfactant Sci Ser 1999, 83, 147.
21. Hong, S.; Kim, M.; Hong, C. K.; Jung, D.; Shim, S. E. Synth Metal 2008, 158, 900.
22. Ding, L.; Wang, X.; Gregory, R. V. Synth Metal 1999, 104, 73.
23. Huang, Y.; Jiang, S.; Wu, L.; Hua, Y. Polym Test 2004, 23, 9.
24. Yun, S.; Kim, J. Synth Metal 2007, 157, 523.